Behavioral/Cognitive

Defining Overlooked Structures Reveals New Associations between the Cortex and Cognition in Aging and Alzheimer's Disease

Samira A. Maboudian,[1,2] Ethan H. Willbrand,[3] Joseph P. Kelly,[4] William J. Jagust,[1,2,5] and Kevin S. Weiner,[1,2,6] for the Alzheimer's Disease Neuroimaging Initiative*

[1]Helen Wills Neuroscience Institute, University of California Berkeley, Berkeley, California 94720, [2]Department of Neuroscience, University of California Berkeley, Berkeley, California 94720, [3]School of Medicine and Public Health, University of Wisconsin-Madison, Madison, Wisconsin 53726, [4]Department of Medical Social Sciences, Feinberg School of Medicine, Northwestern University, Chicago, Illinois 60611, [5]Molecular Biophysics and Integrated Bioimaging, Lawrence Berkeley National Laboratory, Berkeley, California 94720, and [6]Department of Psychology, University of California Berkeley, Berkeley, California 94720

Recent work suggests that indentations of the cerebral cortex, or sulci, may be uniquely vulnerable to atrophy in aging and Alzheimer's disease (AD) and that the posteromedial cortex (PMC) is particularly vulnerable to atrophy and pathology accumulation. However, these studies did not consider small, shallow, and variable tertiary sulci that are located in association cortices and are often associated with human-specific aspects of cognition. Here, we manually defined 4,362 PMC sulci in 432 hemispheres in 216 human participants (50.5% female) and found that these smaller putative tertiary sulci showed more age- and AD-related thinning than larger, more consistent sulci, with the strongest effects for two newly uncovered sulci. A model-based approach relating sulcal morphology to cognition identified that a subset of these sulci was most associated with memory and executive function scores in older adults. These findings lend support to the retrogenesis hypothesis linking brain development and aging and provide new neuroanatomical targets for future studies of aging and AD.

Key words: **aging; Alzheimer's disease; neuroanatomy; neuroimaging; tertiary sulci**

Significance Statement

Large-scale changes in cortical structure in aging suggest sulci are particularly vulnerable to atrophy. However, tertiary sulci, the smallest and most individually variable cortical folds associated with cognitive development, have not been studied in aging. Here, we investigate tertiary sulci for the first time in aging and Alzheimer's disease (AD). We find that these smaller and shallower sulci show more age- and AD-related thinning than larger sulci in the posteromedial cortex (PMC) and that the atrophy of a subset of PMC sulci is most associated with cognition in older adults. These findings support classical theories linking developmental and aging trajectories at a novel anatomical resolution and provide insight into relationships between individual differences in structural brain changes and cognitive decline.

Received Sept. 10, 2023; revised Jan. 5, 2024; accepted Jan. 27, 2024.

Author contributions: S.A.M., W.J.J., and K.S.W. designed research; S.A.M., E.H.W., J.P.K., W.J.J., and K.S.W. performed research; S.A.M. analyzed data; S.A.M., W.J.J., and K.S.W. wrote the paper.

*Data used in this article were obtained from the Alzheimer's Disease Neuroimaging Initiative (ADNI) database (adni.loni.usc.edu). ADNI investigators thus contributed to the design and implementation of ADNI and/or provided data but did not participate in analysis or writing of this report. A complete list of ADNI investigators can be found at http://adni.loni.usc.edu/wp-content/uploads/how_to_apply/ADNI_Acknowledgement_List.pdf.

This research was supported by a National Institutes of Health (NIH) T32 training Grant 2T32NS095939-06 (to S.A.M.), a Medical Scientist Training Program Grant T32 GM140935 (to E.H.W.), and an National Science Foundation CAREER Award 2042251 (to K.S.W.).

Alzheimer's Disease Neuroimaging Initiative: Data collection and sharing for this project was funded by ADNI (National Institutes of Health Grant U01 AG024904) and DOD ADNI (Department of Defense Award W81XWH-12-2-0012). ADNI is funded by the National Institute on Aging and the National Institute of Biomedical Imaging and Bioengineering and through contributions from the following: AbbVie, Alzheimer's Association, Alzheimer's Drug Discovery Foundation, Araclon Biotech, BioClinica, Biogen, Bristol-Myers Squibb, CereSpir, Cogstate, Eisai, Elan Pharmaceuticals, Eli Lilly and Company, EuroImmun, F. Hoffmann-La Roche and its affiliated company Genentech, Fujirebio, GE HealthCare, IXICO, Janssen Alzheimer Immunotherapy Research & Development, Johnson & Johnson Pharmaceutical Research & Development, Lumosity, Lundbeck, Merck & Co, Meso Scale Diagnostics, NeuroRx Research, Neurotrack Technologies, Novartis Pharmaceuticals, Pfizer, Piramal Imaging, Servier, Takeda Pharmaceuticals, and Transition Therapeutics. The Canadian Institutes of Health Research is providing funds to support ADNI clinical sites in Canada. Private sector contributions are facilitated by the Foundation for the National Institutes of Health (www.fnih.org). The grantee organization is the Northern California Institute for Research and Education, and the study is coordinated by the Alzheimer's Therapeutic Research Institute at the University of Southern California. ADNI data are disseminated by the Laboratory for Neuro Imaging at the University of Southern California.

Human Connectome Project (HCP): Young adult neuroimaging data were provided by the HCP, WU-Minn Consortium (PIs: David Van Essen and Kamil Ugurbil; NIH Grant 1U54-MH-091657) funded by the 16 NIH Institutes and Centers that support the NIH Blueprint for Neuroscience Research and the McDonnell Center for Systems Neuroscience at Washington University.

The authors declare no competing financial interests.

Correspondence should be addressed to Samira A. Maboudian at smaboudian@berkeley.edu.

https://doi.org/10.1523/JNEUROSCI.1714-23.2024

Introduction

Understanding relationships between structural brain changes and cognitive decline in aging is a fundamental objective of aging research. Findings from large-scale, group-level atrophy studies with hundreds of participants converge on broadly consistent patterns across lobes (Raz et al., 1997; Salat et al., 2004; Du et al., 2007; Fjell et al., 2009a,b); however, more specific investigations of individual differences are less clear. Measuring changes in sulci in aging has been proposed to explore individual differences in cortical structure without biases introduced from a common stereotaxic space (Mangin et al., 2004; Bertoux et al., 2019) and to provide additional insights beyond regional volume and thickness analyses, since sulcal morphology is thought to reflect underlying white matter architecture (Van Essen, 2020; Voorhies et al., 2021). Such studies in aging have found that sulci are more vulnerable to thinning than gyri (Lin et al., 2021) and that sulcal morphology is related to cognitive decline (Liu et al., 2011; Mortamais et al., 2022). In Alzheimer's disease (AD), sulcal morphology has been found to be related to cognitive impairment and is more diagnostically accurate than traditional measures like hippocampal volume (Hamelin et al., 2015; Bertoux et al., 2019).

These studies have focused on the largest, deepest sulci. However, an emerging area of investigation is the role of tertiary sulci: the smallest, shallowest indentations that appear latest in development and most recently in primate evolution (Sanides, 1964; Miller et al., 2021; Miller and Weiner, 2022). The morphology of tertiary sulci is associated with individual differences in cognitive development (Voorhies et al., 2021; Willbrand et al., 2022b; Yao et al., 2022) and with symptoms and onset of disorders including schizophrenia (Garrison et al., 2015) and frontotemporal dementia (Harper et al., 2022). To our knowledge, no prior research has examined sulcal morphology including tertiary sulci in normal aging or AD.

Here, we build on these findings to investigate tertiary sulci in the aging brain for the first time. One reason tertiary sulci have been overlooked is that they often do not appear in analyses averaged across individuals and are not automatically identified by common cortical parcellations (Miller et al., 2021; Voorhies et al., 2021). Consequently, tertiary sulci must be manually identified in each hemisphere by trained raters (Chiavaras and Petrides, 2000; Garrison et al., 2015; Amiez et al., 2018, 2019, 2023; Lopez-Persem et al., 2019; Voorhies et al., 2021; Harper et al., 2022; Willbrand et al., 2022b, 2023c). Because this process is laborious, studies commonly restrict analyses to a single sulcus or region. Here, we focus on the posteromedial cortex (PMC). PMC, which includes the precuneus and posterior cingulate (Parvizi et al., 2006; Willbrand et al., 2022a; Foster et al., 2023), is vulnerable to age-related atrophy (Fjell et al., 2009a,b) and functional connectivity alterations that correlate with cognitive impairment (Andrews-Hanna et al., 2007; Leech and Sharp, 2014; Edde et al., 2020). In AD, PMC is also vulnerable to atrophy (Du et al., 2007; Pengas et al., 2010) and is one of the earliest sites of pathological amyloid-β (Aβ) accumulation (Buckner et al., 2009; Vannini et al., 2013) and tau spread beyond the medial temporal lobe (Braak and Braak, 1991; Harrison et al., 2019).

This study investigates changes in the morphology of PMC sulci in young adults (YAs), healthy older adults (OAs), and older adults with AD, guided by the following questions: (1) Are morphological changes uniform in PMC sulci, or are particular sulci or sulcal types uniquely vulnerable? (2) Is there a relationship between PMC sulcal morphology and cognition in older adults, and is this relationship specific to certain sulci? Answering these questions is theoretically meaningful: the retrogenesis model of aging and AD suggests brain aging and degeneration mirrors development, first affecting evolutionarily newer and later developing areas and, thus, leading to declines in higher-order cognitive processes (Reisberg et al., 1999). Consequently, we hypothesize that tertiary sulci may be particularly vulnerable to aging- or AD-related degeneration and subsequent cognitive decline.

Materials and Methods

Participants

Young adults. Data for the YA cohort analyzed in this study are from the Human Connectome Project Young Adult (HCP-YA) database (https://www.humanconnectome.org/study/hcp-young-adult/overview; Van Essen et al., 2013). We used data from 72 randomly selected participants (36 female; age, 22–36; $\mu = 29.1$ years; Table 1). HCP consortium data were previously acquired using protocols approved by the Washington University Institutional Review Board. In this study, we have used the same participants as in our prior work delineating sulcal morphology in human and chimpanzee PMC (Willbrand et al., 2023c).

Older adults. Data for the older adult cohorts analyzed in this study are from the Alzheimer's Disease Neuroimaging Initiative (ADNI; https://adni.loni.usc.edu/). We used MRI scans from 144 older adults: 72 classified as cognitively normal OAs and 72 with a diagnosis of AD, based on ADNI protocol criteria (Petersen et al., 2010). The 72 OA participants were randomly chosen from the subset of cognitively normal OAs in ADNI (38 female; age, 65–90; $\mu = 76.0$ years; Table 1). The 72 AD participants were chosen from the subset of adults with AD in ADNI who had an MRI and Aβ PET scan within the same year, such that the OA and AD groups were age matched (35 female; age, 65–89; $\mu = 76.2$ years; Table 1). All AD participants were confirmed to be Aβ positive based on ADNI's Aβ PET cortical summary SUVR positivity thresholds (Landau et al., 2012; Royse et al., 2021).

Data acquisition

MRI: young adults. Anatomical T1-weighted MRI scans (0.8 mm voxel resolution) were obtained in native space from the HCP database, as were outputs from the HCP-modified FreeSurfer pipeline (v5.3.0; Dale et al., 1999; Fischl et al., 1999a,b; Glasser et al., 2013). Additional details on image acquisition parameters and HCP-specific image processing can be found in Glasser et al. (2013).

MRI: older adults. Anatomical T1-weighted MPRAGE anatomical scans were obtained from the ADNI online repository (http://adni.loni.usc.edu). The resolution and exact scanning parameters varied slightly across the sample (see Extended Data Tables 1-1 and 1-2 for scanning parameters), but ADNI imaging protocols have been standardized to minimize variance across sites (Jack et al., 2008). Each scan was visually inspected for scanner artifacts, and then cortical surface reconstructions were generated for each participant using the standard FreeSurfer processing pipeline [FreeSurfer (v6.0.0): surfer.nmr.mgh.harvard.edu; Dale et al., 1999; Fischl et al., 1999a].

Cognitive data. Cognitive data were obtained from ADNI for OA and AD groups. We used the ADNI memory (ADNI-Mem) composite

Table 1. Summary of participant characteristics

Group	Age: range (μ, SD)	Sex: %F	Years of Edu: μ (SD)	CDR SOB: μ (SD)	Aβ status: % Aβ+
YA	22–36 (29.06, 3.57)	50.0			
OA	65–90 (76.01, 6.32)	52.8	16.47 (2.25)	0.1 (0.5)	51%
AD	65–89 (76.15, 5.89)	48.6	15.74 (2.32)	4.4 (1.8)	100%

Characteristics of participant samples from the HCP-YA and the ADNI databases. Aβ status and Clinical Dementia Rating Scale Sum of Boxes (CDR SOB) were only available in the OA and AD groups, and years of education (Edu) is only reported for older adult groups because only OAs and ADs are considered in cognition analyses. For scanning parameters, see Extended Data Tables 1-1 and 1-2.

score from the ADNI neuropsychological battery (Crane et al., 2012) as a measure of memory performance and ADNI executive function (ADNI-EF) composite score as a measure of executive function (Gibbons et al., 2012).

Manual sulcal labeling of PMC sulci

For both cohorts, each cortical reconstruction obtained by the steps above was inspected for segmentation errors (which were manually corrected if necessary). All sulcal labeling and extraction of anatomical metrics were calculated from the FreeSurfer cortical surface reconstructions of individual participants.

As in our prior work (Willbrand et al., 2022a, 2023c), we defined PMC sulci for each participant based on the most recent schematics of sulcal patterning by Petrides (2019) as well as their own pial, inflated, and smoothed white matter (smoothwm) FreeSurfer surfaces. In some cases, the precise start or end point of a sulcus can be difficult to determine on a surface (Borne et al., 2020); examining consensus across multiple surfaces allowed us to clearly determine each sulcal boundary in each individual. Sulci were defined in *tksurfer*, where manual lines were drawn on each participant's FreeSurfer inflated cortical surface to distinguish sulci. For each hemisphere, the location of PMC sulci was identified by trained raters (S.A.M., E.H.W.) and confirmed by an expert neuroanatomist (K.S.W.) in agreement with an established atlas (Petrides, 2019) and our prior work identifying sulci in this area (Willbrand et al., 2022a, 2023c). See Extended Data Figure 1-1 for all sulcal labels on all OA and AD hemispheres and our prior work for all YA labels and a more in-depth description of sulcal anatomy in PMC (Willbrand et al., 2023c).

For this process, we started with the largest and deepest sulci that bound our region of interest (PMC): the parieto-occipital sulcus (pos) posteriorly and the marginal ramus of the cingulate sulcus (mcgs) anteriorly. Next, the splenial sulcus (spls) separates two commonly delineated subregions of PMC: the precuneus (PrC) superiorly and the posterior cingulate cortex (PCC) inferiorly (Vogt et al., 1995; Willbrand et al., 2022a, 2023c). PrC contains four consistent sulci: the dorsal precuneal limiting sulcus (prculs-d) and three precuneal sulci (posterior, prcus-p; intermediate, prcus-i; anterior, prcus-a). PCC contains one consistent sulcus: the inframarginal sulcus (ifrms). In addition to these eight consistent sulci in PMC, there are four variably present sulcal indentations: the ventral precuneal limiting sulcus (prculs-v) in PrC, the posterior intracingulate sulcus (icgs-p) in PCC anterior to the ifrms, and the dorsal and ventral subsplenial sulci (sspls-d and sspls-v, respectively) inferior to the spls. For more detail, see our prior work characterizing PMC sulcal morphology (Willbrand et al., 2023c) and Figure 1 for example participant hemispheres with PMC sulci defined.

Sulcal probability maps

As in prior studies (Miller et al., 2021; Voorhies et al., 2021; Willbrand et al., 2023b), sulcal probability maps were generated to display the vertices of highest correspondence across participants for each sulcus. Each sulcal label in every participant was mapped from the individual's surface to the *fsaverage* surface; from there, for each vertex, we calculated the proportion of participants for whom the vertex is labeled as a given sulcus, and the sulcus with the highest overlap was assigned to each vertex. To improve visual interpretability, we generated maximum probability maps (MPMs) for each sulcus by constraining each map to 10% overlap across participants (Fig. 1*B*), as done previously (Willbrand et al., 2023b). Maps were generated separately for each group (YA, OA, and AD), and both the 10% thresholded MPMs and the unthresholded maps are provided. The centroid coordinate of each 10% thresholded MPM displayed in Freeview on the *fsaverage* surface is given in Table 2 and Extended Data Table 2-1.

Quantification of sulcal morphology

For this study, we extracted and analyzed the cortical thickness and depth of each PMC sulcus, as these are two defining morphological features of cortical sulci (Fischl and Dale, 2000; Goghari et al., 2007; Vandekar et al., 2015; Miller et al., 2021; Demirci and Holland, 2022) that are also of interest in aging (Jin et al., 2018; Shen et al., 2018; Madan, 2019; Lin et al., 2021; Tang et al., 2021). When comparing across groups (YA, OA, AD), cortical thickness is used as a measure of atrophy, as is common in prior literature (Salat et al., 2004; Lindroth et al., 2019). Though prior work examining sulcal morphology in aging has also studied sulcal width (Liu et al., 2011, 2013; Hamelin et al., 2015; Jin et al., 2018; Bertoux et al., 2019; Tang et al., 2021; Mortamais et al., 2022), we found that the current toolbox that extracts this information from individual sulcal labels in FreeSurfer (Madan, 2019) failed to obtain the width of many smaller sulci (previous studies only examine large sulci). Therefore, we were not able to examine sulcal width in the present study.

Cortical thickness. Cortical thickness (in millimeters) was generated for each sulcus using the *mris_anatomical_stats* function in FreeSurfer (Dale et al., 1999; Fischl et al., 1999a). Raw (un-normalized) cortical thickness values (in millimeters) are used in the present study as previous studies showed that raw, un-normalized values outperform normalized measures of thickness in MCI and AD (Westman et al., 2013).

Depth. Sulcal depth was calculated from the native cortical surface reconstruction, measuring from the sulcal fundus to the smoothed outer pial surface. Raw values for sulcal depth (in millimeters) were calculated using a modified version of an algorithm for robust morphological statistics that builds on the FreeSurfer pipeline (Madan, 2019).

Experimental design and statistical analyses

To compare the cortical thickness of PMC sulci between groups, we ran a linear mixed-effects model (LME) with the following predictors: group (YA, OA, AD), sulcus, and hemisphere (left or right) and their interactions. Group, hemisphere, and sulcus were considered fixed effects, and for random effects sulcus was nested within the hemisphere, which was nested within subjects. ANOVA *F*-tests were applied to each model. We also repeated these analyses with sulcal depth instead of cortical thickness. For all post hoc comparisons conducted, p values were corrected for multiple comparisons with Tukey's method, and the Tukey-corrected p is reported.

To determine which sulcal measures were most associated with cognition, we employed a least absolute shrinkage and selection operator (LASSO) regression, as described previously (Voorhies et al., 2021; Yao et al., 2022). We utilize LASSO regression as a form of feature selection to determine whether the cortical thickness of any PMC sulci in particular predicts memory (ADNI-Mem) scores. We employ this method separately for each hemisphere and combined across both hemispheres. LASSO regression requires all individuals to have the same predictors; therefore, in order to include more than one small, shallow sulcus while maximizing the available sample size, we included the cortical thickness of all eight consistent sulci (pos, prculs-d, prcus-p, prcus-i, prcus-a, spls, mcgs, ifrms) plus the next most consistent PMC sulcus (sspls-v, present in 61.1% of hemispheres). This resulted in 106 individuals with all 9 of these sulci in the left hemisphere and 70 with all 9 in the right for the LASSO regressions. OA and AD participants were combined to increase the range of scores and sample size available (Extended Data Fig. 5-1). For the ADNI-EF analyses, one participant with all nine sulci in the left hemisphere was excluded from analyses because they were missing the ADNI-EF composite score.

This approach allows for data-driven variable selection: LASSO algorithms penalize model complexity by applying a shrinking parameter (α) to the absolute magnitudes of the coefficients, dropping the lowest from the model. LASSO regression increases model generalizability by providing a sparse solution that reduces coefficient values and decreases variance in the model, without increasing bias (Heinze et al., 2018). To choose the optimal value for α, we use the *GridSearchCV* function of the *scikit-learn* Python module to perform an exhaustive search over a range of values, selecting the value that minimizes the cross-validated mean squared error (MSE_{CV}) using the following formula:

$$y_i = \beta_0 + \beta_1\ \mathrm{pos} + \beta_2\ \mathrm{prculs\_}d + \beta_3\ \mathrm{prcus\_}p + \beta_4\ \mathrm{prcus\_}i + \beta_5\ \mathrm{prcus\_}a + \beta_6\ \mathrm{spls} + \beta_7\ \mathrm{mcgs} + \beta_8\ \mathrm{ifrms} + \beta_9\ \mathrm{sspls\_}v + \varepsilon_i \quad (1)$$

From the LASSO regression with the optimal α value, we identify our model of interest, which best explains memory scores from a subset of

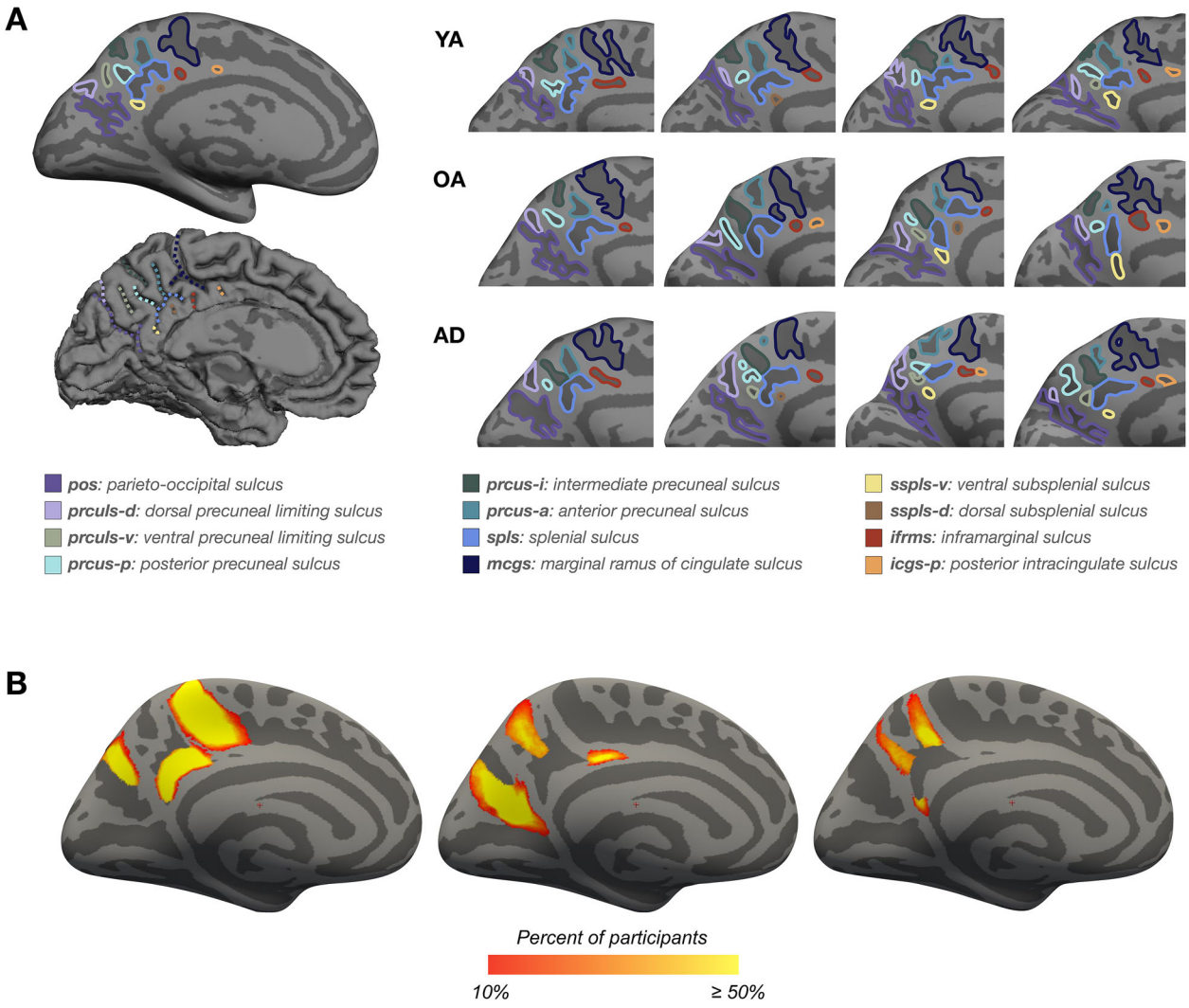

Figure 1. PMC sulcal labels in example hemispheres and average probability maps. ***A***, Left, An inflated (top) and pial (bottom) cortical surface reconstruction of an individual human hemisphere; sulci are dark gray and gyri light gray. Individual PMC sulci are colored according to the legend. Right, Four example hemispheres within each group, zoomed in to the PMC and depicting variability in sulcal incidence between participants (9–12 sulci per hemisphere: 8 consistent, 4 variably present). Right hemisphere images are mirrored so that all images are in the same orientation for comparison. See Extended Data Figure 1-1 for all OA and AD participant hemispheres with labels. Legend: YA, young adult; OA, cognitively normal older adult; AD, older adult with Alzheimer's. ***B***, MPMs for nine example sulci (3 per image) generated using all participants' sulcal labels projected to the left hemisphere *fsaverage* surface. At each vertex, maps indicate the proportion of participants for whom that vertex is labeled as a given sulcus (yellow is higher overlap). Sulci shown: prculs-d, spls, and mcgs (left); pos, prcus-i, and ifrms (middle); sspls-v, prcus-p, and prcus-a (right). MPMs generated from all YA participants' labels are shown, but MPMs generated from all three groups (YA, OA, and AD) are available for download and can be projected from *fsaverage* onto individual participant surfaces (see Materials and Methods, Code and data accessibility).

the original predictors. One model was identified per hemisphere as follows:

$$\text{Right hemisphere: } y_i = \beta_0 + \beta_1\ \text{prculs\_}d + \beta_2\ \text{prcus\_}p + \beta_3\ \text{ifrms} + \beta_4\ \text{sspls\_}v + \varepsilon_i \quad (2)$$

$$\text{Left hemisphere: } y_i = \beta_0 + \beta_1\ \text{pos} + \beta_2\ \text{prcus\_}p + \beta_3\ \text{spls} + \beta_4\ \text{sspls\_}v + \varepsilon_i \quad (3)$$

We also combined sulcal measures across both hemispheres in a separate LASSO regression. Additionally, to determine whether any of these sulcal measures remain as predictors in the model when also accounting for group status (OA or AD), we added group as a predictor to the LASSO regression, which resulted in the following final model:

$$y_i = \beta_0 + \beta_1\ \text{Group} + \beta_2\ \text{prcus\_}p\text{\_RH} + \beta_3\ \text{ifrms\_RH} + \beta_4\ \text{sspls\_}v\text{\_RH} + \beta_5\ \text{spls\_RH} + \beta_6\ \text{sspls\_}v\text{\_LH} + \varepsilon_i \quad (4)$$

We use linear regression with leave-one-out cross-validation (LOOCV) in order to compare various models; all regression models were implemented with the *scikit-learn* module. To verify that the results of our feature selection [(2) and (3)] outperform a full model containing all PMC sulci [(1)], we compare the simplified models of interest with the full model, separately for each hemisphere. We also compared models (2) and (3) to determine which hemisphere provided the best predictive power. To determine model specificity, we investigated whether the observed relationship between sulci and task performance generalized to other cognitive domains or morphological features: we compared the original models to models predicting ADNI-EF scores instead of ADNI-Mem scores from sulcal thickness and to models using the depth of selected sulci as the predictors instead of cortical thickness. We compared the fits of all models of interest using the Akaike information criterion (AIC). An AIC > 2 suggests an interpretable difference between models, and AIC > 10 suggests a strong difference between models (lower AIC suggests better model fit).

To determine if available covariates (age, education, and sex, summarized in Table 1) were associated with ADNI-Mem scores, we calculated

Table 2. Centroid coordinates of young adult sulcal MPMs

Sulcus	Centroid R, A, S (left hemi)	Centroid R, A, S (right hemi)
pos	−21.75, −63.54, 21.06	23.02, −60.00, 22.21
mcgs	−18.02, −39.94, 48.91	16.84, −37.92, 49.79
prculs-d	−11.92, 68.81, 37.03	13.08, −69.36, 39.40
spls	−11.06, −47.56, 29.62	10.96, −47.05, 30.66
prcus-a	−8.02, −50.96, 48.11	7.23, −48.90, 49.19
prcus-i	−11.52, −57.90, 46.77	6.91, −58.28, 47.39
prcus-p	−6.82, −63.23, 36.77	5.96, −61.61, 36.83
prculs-v	−4.76, −62.44, 25.17	5.37, −59.97, 28.56
sspls-v	−6.69, −53.04, 13.52	6.53, −50.76, 15.28
icgs-p	−3.98, −17.39, 36.50	4.21, −17.10, 36.99
ifrms	−4.94, −28.5, 35.5	5.39, −28.69, 36.13
sspls-d	−4.82, −44.21, 26.70	5.01, −45.00, 25.74

Centroid coordinates of the 10% thresholded MPM for each sulcus in the young adult group, in *fsaverage* RAS coordinates. The centroid coordinates for both older adult groups (OA and AD) are given in Extended Data Table 2-1.

Person correlations (r_p) between age or education and ADNI-Mem scores, and *t* tests comparing ADNI-Mem scores between male and female participants.

Packages used for statistical analysis

All statistical tests were implemented in Python (v3.9.13) and R (v4.2.2). For morphological comparisons, LMEs were implemented with the *lme* function from the *nlme* R package. ANOVA *F* tests were implemented with the *anova* function from the built-in *stats* R package, and the effect sizes for ANOVA effects are reported as partial eta-squared (η_P^2) values computed with the *eta_squared* function from the *effectsize* R package. Post hoc analyses on ANOVA effects and effect sizes were computed with the *emmeans*, *contrast*, and *eff_size* functions from the *emmeans* R package (*p* values adjusted with Tukey's method). Correlations were computed with the *spearmanr* (r_s) or *pearsonr* (r_p) function from the *stats* module of the Python *SciPy* package (v1.9.1), and two-sided *t* tests were performed with the *ttest_ind* function from *SciPy.stats*. LASSO regression was implemented using the *scikit-learn* Python module (v1.0.2).

Code and data accessibility

Code and data used for this project, including sulcal probability maps that can be downloaded and projected from *fsaverage* onto individual participant surfaces, will be made freely available on GitHub upon publication at the following link: https://github.com/cnl-berkeley/stable_projects/tree/main/PMCSulcalMorphology_AgingAD. The colorblind-friendly color schemes used in our figures were created using the toolbox available at https://davidmathlogic.com/colorblind/. Requests for further information should be directed to the corresponding author.

Results

Small, shallow sulci show more age- and AD-related thinning, with the strongest effects for newly uncovered sulci (ifrms and sspls-v)

We first manually defined 4,362 PMC sulci in 432 hemispheres in 216 adult participants in three groups: 72 YAs aged 22–36, 72 cognitively normal OA aged 65–90, and 72 adults with AD aged 65–89 (age matched to OA). Previous work shows that this sample size is sufficient to quantify reproducible and reliable results relating sulcal morphology to cognition in individual participants (Garrison et al., 2015; Borst et al., 2016; Cachia et al., 2017; Lopez-Persem et al., 2019; Voorhies et al., 2021; Willbrand et al., 2022b, 2023a; Yao et al., 2022). PMC sulci were manually defined on the cortical surface reconstruction of each participant's T1-weighted MRI scan according to the most recent comprehensive sulcal atlas (Petrides, 2019; Fig. 1) as in our previous studies (Willbrand et al., 2022a, 2023c; see Materials and Methods for specifics). In order to assist in identifying PMC sulci in future studies, we provide probabilistic maps of the location of all sulci included in this work in *fsaverage* space generated by calculating the proportion of participants for whom each vertex belongs to a given sulcal label when mapped to *fsaverage* (Fig. 1*B*; Materials and Methods, Code and data accessibility). These maps can be thresholded and projected onto individual participant surfaces to serve as a guide for manual sulcal definitions. Additionally, we provide the coordinates (in *fsaverage* RAS space) for the centroid of each label's map (Table 2 and Extended Data Table 2-1) that can be transformed to MNI or Talairach coordinates.

Sulci are generally categorized as primary, secondary, or tertiary based on their emergence in gestation (Chi et al., 1977; Welker, 1990; Armstrong et al., 1995; Zilles et al., 2013). However, in this study, several sulci are defined (based on our previous work; Willbrand et al., 2022a, 2023c) that are not included in studies describing gestational sulcation patterns. Therefore, we focus on individual-level sulcal analyses agnostic to sulcal-type groupings and instead categorize sulci as smaller and shallower (sulcal depth and area are highly correlated, in our sample $r_p = 0.86$) or larger and deeper; tertiary sulci are typically the smallest and shallowest (Sanides, 1964; Miller et al., 2021; Miller and Weiner, 2022).

To quantify the effects of sulcal thinning in PMC across groups and hemispheres, we ran an LME model with group (YA, OA, AD), sulcus, and hemisphere (left or right) as predictors, including all interactions (Fig. 2*A*). ANOVA *F* tests were applied to each model. We observed a main effect of group ($F_{(2,213)} = 177.31$; $p < 0.0001$; $\eta_P^2 = 0.62$), sulcus ($F_{(11,3864)} = 560.02$; $p < 0.0001$; $\eta_P^2 = 0.61$), and hemisphere ($F_{(1,213)} = 6.60$; $p = 0.011$; $\eta_P^2 = 0.03$, in which right hemisphere sulci were thicker), as well as group × sulcus ($F_{(22,3864)} = 10.41$; $p < 0.0001$; $\eta_P^2 = 0.06$) and group × hemisphere interactions ($F_{(2,213)} = 3.67$; $p = 0.027$; $\eta_P^2 = 0.03$). Post hoc tests revealed that each pairwise group comparison was significant ($p < 0.0001$), with YA having thicker sulci than OA, and OA thicker than AD; each pairwise group comparison was also significant for each hemisphere separately (all $p < 0.0001$), but group differences were slightly greater in the right hemisphere for the YA–OA difference and in the left hemisphere for the OA–AD difference. Within each sulcus, pairwise group comparisons were significant ($p < 0.05$), except for icgs-p ($p = 0.12$), mcgs ($p = 0.24$), and prcus-a ($p = 0.30$) for the OA–AD comparison and sspls-v for the YA–OA comparison ($p = 0.10$; see Table 3 for all *p* values and effect sizes).

The strongest effects occurred in small, shallow sulci: the ifrms for the OA–YA comparison and the sspls-v for the AD–OA comparison (Table 3). Interestingly, the ifrms was recently shown to be the locus of the thickest portion in PMC (Willbrand et al., 2022a), and both the ifrms and sspls-v were recently uncovered and have not been investigated in prior studies of aging (Willbrand et al., 2023c). Additionally, if PMC sulci are split into the "shallowest" (<5 mm) and "deepest" (>5 mm) sulci, the same LME above can be run with depth type (shallow or deep) as a factor instead of sulcal label: that is, the model includes group (YA, OA, AD), depth type (shallow or deep), and hemisphere (left or right) as predictors, including all interactions. With this model, we still observed a main effect of group ($F_{(2,213)} = 173.36$; $p < 0.0001$; $\eta_P^2 = 0.62$) and hemisphere ($F_{(1,213)} = 4.96$; $p < 0.05$; $\eta_P^2 = 0.02$, in which right hemisphere sulci were thicker), as well as an effect of depth type ($F_{(1,426)} = 3382.84$; $p < 0.0001$; $\eta_P^2 = 0.89$) and a group × depth-type interaction ($F_{(2,426)} = 37.61$; $p < 0.0001$; $\eta_P^2 = 0.15$). Post hoc tests of this interaction show that while all group contrasts in thickness are significant for both depth groups (deep and shallow; all $p < 0.001$), the group contrasts are greater for the shallower sulci.

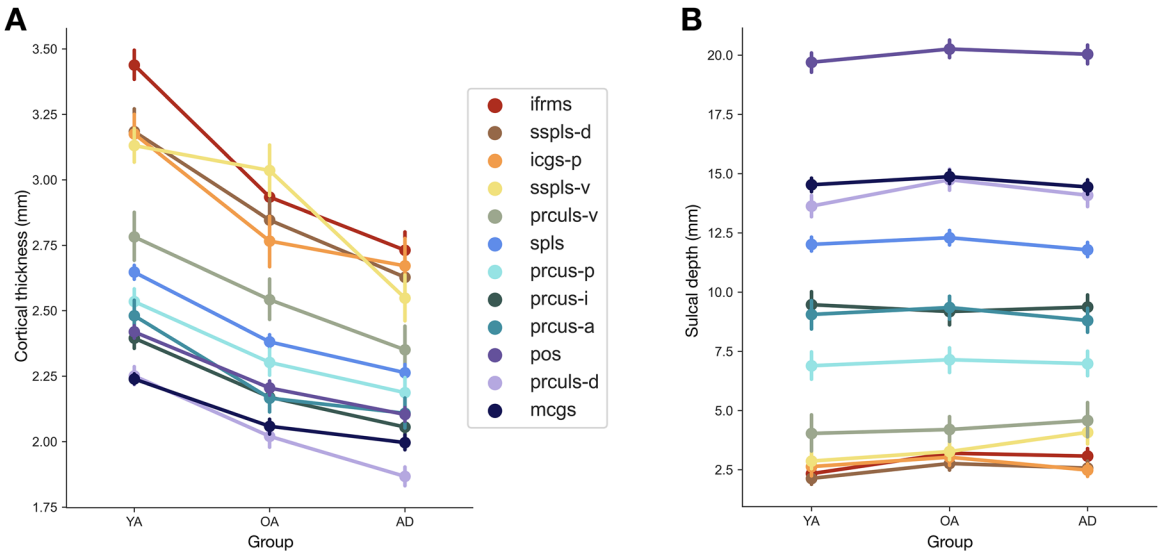

Figure 2. Cortical thickness and sulcal depth differences across groups show the most prominent effects in the thinning of the small, shallow sulci. ***A***, Sulcal cortical thickness (in mm) across groups (YA, younger adult; OA, cognitively normal older adult; AD, older adult with Alzheimer's disease) by sulcus. An LME model with group (YA, OA, AD), sulcus, and hemisphere (left or right) and their interactions as predictors shows a main effect of group ($p < 0.0001$), sulcus ($p < 0.0001$), and hemisphere ($p < 0.05$), as well as a group × sulcus interaction ($p < 0.0001$) and a group × hemisphere interaction ($p < 0.05$). Results of post hoc tests are summarized in Table 3. The points represent the mean thickness, while vertical bars represent the bootstrap 95% CI. ***B***, Sulcal depth (in mm) across groups (YA, younger adult; OA, cognitively normal older adult; AD, older adult with Alzheimer's disease) by sulcus. A LME model with group (YA, OA, AD), sulcus, and hemisphere (left or right) and their interactions as predictors shows a main effect of group ($p = 0.01$), sulcus ($p < 0.0001$), and hemisphere ($p < 0.0001$), as well as a group × sulcus interaction ($p < 0.05$) and a sulcus × hemisphere interaction ($p < 0.0001$).

Table 3. Results of post hoc tests for LME models of cortical thickness

Sulcus	Group comparison	Estimate	*t* ratio	Effect size (Cohen's *d*)	*p* value
sspls-d	OA-YA	−0.3596	−6.860	**−5.259**	**<0.0001**
	AD-OA	−0.1975	−3.624	**−2.888**	**0.001**
ifrms	OA-YA	−0.5031	−13.017	**−7.357**	**<0.0001**
	AD-OA	−0.2041	−5.275	**−2.985**	**<0.0001**
icgs-p	OA-YA	−0.3946	−8.437	**−5.771**	**<0.0001**
	AD-OA	−0.0992	−1.987	−1.451	0.12
sspls-v	OA-YA	−0.0964	−2.052	−1.410	0.10
	AD-OA	−0.4956	−10.354	**−7.248**	**<0.0001**
prculs-v	OA-YA	−0.2578	−4.897	**−3.770**	**<0.0001**
	AD-OA	−0.1839	−3.564	**−2.689**	**0.0013**
prcus-p	OA-YA	−0.2324	−6.021	**−3.398**	**<0.0001**
	AD-OA	−0.1154	−2.989	**−1.687**	**0.009**
prcus-a	OA-YA	−0.3147	−8.155	**−4.603**	**<0.0001**
	AD-OA	−0.0578	−1.494	−0.845	0.30
prcus-i	OA-YA	−0.2252	−5.835	**−3.293**	**<0.0001**
	AD-OA	−0.1143	−2.962	**−1.672**	**0.0095**
spls	OA-YA	−0.2663	−6.899	**−3.894**	**<0.0001**
	AD-OA	−0.1179	−3.056	**−1.725**	**0.007**
prculs-d	OA-YA	−0.2307	−5.976	**−3.373**	**<0.0001**
	AD-OA	−0.1531	−3.967	**−2.239**	**<0.001**
mcgs	OA-YA	−0.1803	−4.670	**−2.636**	**<0.0001**
	AD-OA	−0.0622	−1.612	−0.910	0.24
pos	OA-YA	−0.2143	−5.552	**−3.133**	**<0.0001**
	AD-OA	−0.1013	−2.624	**−1.481**	**0.025**

Results from post hoc comparisons for the LME model comparing the cortical thickness of every PMC sulcus (Fig. 2*A*), calculated with *emmeans* in R. Significant group comparisons (Tukey-adjusted $p < 0.05$) are bolded. Sulci are listed in order from shallowest to deepest (based on average depth in YA).

As sulcal depth has been reported to decrease in aging, we ran the same linear LME described above for sulcal depth instead of cortical thickness (Fig. 2*B*), especially because previous results have focused on large, deep primary sulci and have shown mixed results that vary by sulcus (with some sulci showing no decrease in depth with age; Jin et al., 2018; Shen et al., 2018; Madan, 2019; Tang et al., 2021). We observed a significant effect of group ($F_{(2,213)} = 4.67$; $p = 0.010$; $\eta_P^2 = 0.04$), sulcus ($F_{(11,3864)} = 2{,}064.38$; $p < 0.0001$; $\eta_P^2 = 0.85$), and hemisphere ($F_{(1,213)} = 72.60$; $p < 0.0001$; $\eta_P^2 = 0.25$, in which right hemisphere sulci were shallower), and small but significant group × sulcus ($F_{(22,3864)} = 1.65$; $p = 0.029$; $\eta_P^2 = 9.3 \times 10^{-3}$) and hemisphere × sulcus interactions ($F_{(11,3864)} = 8.20$; $p < 0.0001$; $\eta_P^2 = 0.02$). Post hoc tests show the group effect is driven by a difference between YA and OA depth ($p < 0.02$), with the other group comparisons not significant; examining these YA relative to OA group differences at the sulcal level shows they are only significant for prculs-d ($p < 0.001$) and ifrms ($p < 0.02$), with OA sulci deeper in both cases. Examining hemisphere effects by sulcus show that the left hemisphere is deeper than the right ($p < 0.05$) for every sulcus except pos (where right is deeper than the left, $p < 0.001$) and prculs-d (where the hemisphere difference is not significant).

As the ifrms is situated anteriorly in PMC, we tested the hypothesis that there is a relationship between the mean anterior coordinate of each sulcus (using the FreeSurfer RAS coordinate system; see Materials and Methods) and the amount of atrophy in that sulcus across groups (Fig. 3). This quantification showed that the amount of sulcal atrophy was correlated with the anterior coordinate when comparing sulcal cortical thickness differences in aging (between YA and OA; $r^2 = 0.43$; $p < 0.03$), but not when comparing OA and AD ($r^2 = 0.0$; $p > 0.9$). Instead, in AD, there is relatively less atrophy in more anterior sulci and more atrophy in posterior sulci (Fig. 3).

Recently identified small, shallow sulci are most associated with cognition in older adults

To investigate the relationship between PMC sulcal thinning and cognitive decline, we employed a data-driven pipeline described previously (Voorhies et al., 2021; Yao et al., 2022; Willbrand et al., 2023a). We first implemented a LASSO regression model

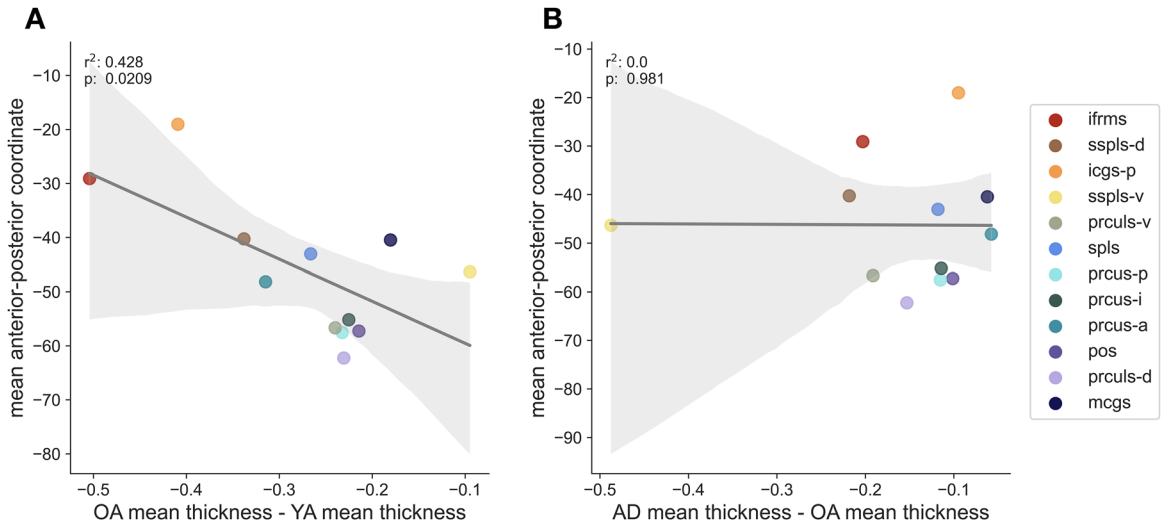

Figure 3. More anterior PMC sulci atrophy most in aging, but this anterior bias is absent in AD. ***A***, Mean anterior–posterior coordinate of each sulcus versus the difference between the average thickness of the sulcus in OA and YA, demonstrating that more anterior sulci are more atrophied in OA. ***B***, Mean anterior–posterior coordinate of each sulcus versus the difference between the average thickness of the sulcus in OA and AD, showing no relationship between anterior–posterior location and atrophy. Sulci colored based on legend (right).

predicting ADNI-Mem composite scores using the sulcal cortical thickness of the nine most common PMC sulci in the sample, separately for each hemisphere (see Materials and Methods). LASSO regression performs feature selection by shrinking model coefficients and removing the lowest from the model, with the sulci that are the strongest predictors of ADNI-Mem scores remaining in the final model. We used LOOCV to determine the value of the LASSO shrinking parameter (α), iteratively fitting models with different α values and choosing the one that minimizes cross-validated mean squared error. This procedure indicates that the thickness of a subset of PMC sulci in each hemisphere is most strongly related to ADNI-Mem scores: pos, prcus-p, spls, and sspls-v in the left hemisphere and prculs-d, prcus-p, ifrms, and sspls-v in the right hemisphere (Fig. 4*A*). Intriguingly, this model identifies recently uncovered small, shallow sulci (ifrms, sspls-v; Willbrand et al., 2022a, 2023c) as explaining a significant amount of variance.

We then assessed the relationship between these LASSO-selected sulci and cognition using linear regression models, in order to compare model performance between hemispheres and across cognitive tasks. Because not all models examined are nested, we compared model performance with the AIC. Lower AIC is better, and $\Delta AIC > 2$ suggests an interpretable difference between models, while $\Delta AIC > 10$ suggests a substantial difference between models.

For each hemisphere, we compared a model predicting ADNI-Mem scores using the thickness of all sulci to a model using the thickness of LASSO-selected sulci (for that hemisphere) only. In the right hemisphere, for the LASSO-selected sulci model, there was a significant association between predicted and actual ADNI-Mem scores ($r_s = 0.55$; $p < 8.2 \times 10^{-7}$; Fig. 4*B*), and the model AIC was −1.99 (Fig. 4*C*). This model outperformed a model with the thickness of all PMC sulci in the right hemisphere (AIC = 18.40; Fig. 4*C*). In the left hemisphere, for the LASSO-selected sulci model, there was also a significant relationship between predicted and actual ADNI-Mem scores ($r_s = 0.41$; $p < 1.1 \times 10^{-5}$; Fig. 4*B*), and the model AIC was 10.17 (Fig. 4*C*). This model outperformed a model with the thickness of all PMC sulci in the left hemisphere (AIC = 30.54; Fig. 4*C*). ΔAIC between the LASSO-selected right hemisphere sulci thickness model and the LASSO-selected left hemisphere sulci model for ADNI-Mem scores is −12.15, indicating that the thickness of right hemisphere LASSO-selected sulci is strongly preferred as a predictor of ADNI-Mem scores over left hemisphere sulci.

We then ran another LASSO regression that included all nine sulci in both hemispheres as well as group (OA or AD) as predictors, in order to examine cross-hemisphere effects and to investigate whether any sulcal thickness measures remain as significant predictors when accounting for group status. Group, as well as a subset of the 18 sulci, was a significant predictor in the final model: right hemisphere sspls-v, ifrms, spls, and prcus-p and left hemisphere sspls-v (Extended Data Fig. 4-1). The AIC for this model was the lowest (−55.05), indicating the best performance with these predictors.

Available covariates (age, education, and sex) were not associated with ADNI-Mem scores (age, $r_p = -0.033$; $p > 0.6$; education, $r_p = 0.12$; $p > 0.14$; sex, $p > 0.14$); unsurprisingly, including them in the model did not improve model AIC in either hemisphere (Fig. 4*C*). Further, even though there were no significant depth effects across groups, in order to determine whether these relationships with cognition apply to other morphological measures beyond thickness, we also assessed the relationship between the depth of the same LASSO-selected sulci in each hemisphere and ADNI-Mem scores. The LASSO-selected sulcal depth model predictions were not correlated with actual ADNI-Mem scores in either hemisphere, and the thickness model was substantially preferred over the depth model in both hemispheres (Extended Data Fig. 4-2).

To determine whether the morphology of these sulci is related to other cognitive domains beyond memory, we also assessed the relationship between the same LASSO-selected sulci in each hemisphere and ADNI-EF scores. In the right hemisphere, for the LASSO-selected sulci model, there was a significant association between predicted and actual ADNI-EF scores ($r_s = 0.48$; $p < 2.2 \times 10^{-5}$; Fig. 5*A*), though this relationship is weaker than with ADNI-Mem scores, and the model AIC was 22.43 (Fig. 5*B*). We compared the model performance between the LASSO-selected sulcal thickness models for ADNI-Mem and ADNI-EF: ΔAIC = −24.41, indicating that the ADNI-Mem

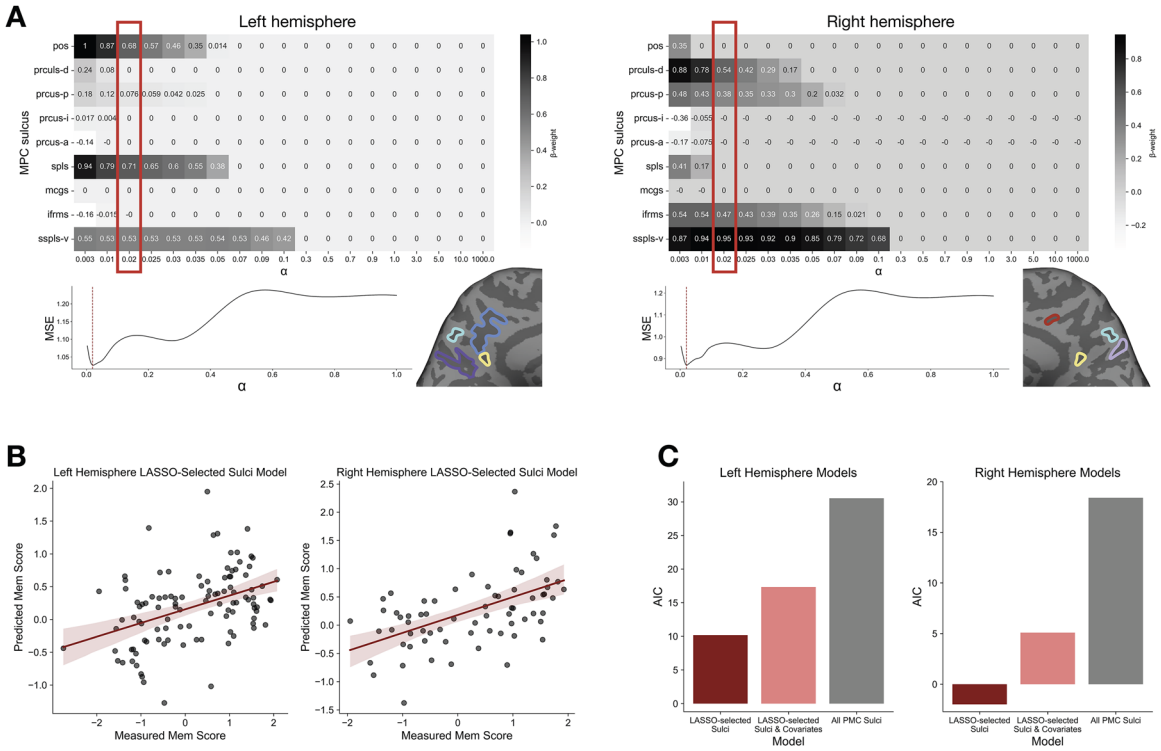

Figure 4. A subset of PMC sulci is most associated with memory scores. ***A***, LASSO regression results for models predicting ADNI-Mem composite scores from left hemisphere (left) and right hemisphere (right) PMC sulcal thickness (for depth models, see Extended Data Fig. 4-2). Top, β-coefficients for each predictor (sulcal cortical thickness) over a range of shrinking parameter (α) values. Red box depicts values for the chosen model (α value that minimizes MSE_{CV}). Bottom left, MSE_{CV} at each α level; α was selected to minimize MSE_{CV} (dotted line). Bottom right, example participant PMC with model-selected sulci highlighted. ***B***, Correlation between actual ADNI-Mem scores and predicted scores from the LOOCV for the best performing LASSO-selected model in the left and right hemispheres, which had the predictors indicated by the red boxes in ***A***. Left, $r_s = 0.41$; $p < 1.1 \times 10^{-5}$; right, $r_s = 0.55$; $p < 8.2 \times 10^{-7}$. ***C***, Model comparison (AIC) of the model with the thickness of sulci selected by the LASSO regression as predictors; a model with the thickness of LASSO-selected sulci and age, sex, and education as predictors; and a model with the thickness of all PMC sulci as predictors for left and right hemispheres. LASSO-selected models have a lower AIC in both hemispheres compared with other models. See Extended Data Figure 4-1 for a model combining both hemispheres.

model is preferred (Fig. 5*B*). In the left hemisphere, for the LASSO-selected sulci thickness model, there was also a significant relationship between predicted and actual ADNI-EF scores ($r_s = 0.40$; $p < 2.8 \times 10^{-5}$; Fig. 5*A*), though again this relationship is weaker than with ADNI-Mem scores, and the AIC was 56.29 (Fig. 5*B*). The ΔAIC between this model and the left hemisphere ADNI-Mem thickness model (ΔAIC = −46.13) indicates that in the left hemisphere, the ADNI-Mem model is again preferred over the ADNI-EF model (Fig. 5*B*). Importantly, despite the preference for the ADNI-Mem model, the significant correlations in both hemispheres for the ADNI-EF model indicate that the relationship between the sulci selected by our original model and cognition generalizes to another cognitive domain.

Discussion

To investigate changes in sulcal morphology in aging and AD at a previously unexplored level of neuroanatomical detail—including recently uncovered sulci presently excluded from neuroanatomical atlases and neuroimaging software packages—we manually defined 4,362 PMC sulci across 432 hemispheres. We find that small, shallow sulci showed the most age- and AD-related thinning. Interestingly, there was an anterior bias for atrophy in aging that is absent in AD. A model-based approach relating sulcal morphology to cognition identified that the thickness of a subset of these sulci (including the two newly identified, small sulci showing the strongest atrophy effects: ifrms and sspls-v) is most associated with memory and executive function scores in OAs, especially in the right hemisphere. Here, we discuss these findings in the context of (1) highlighting the role of tertiary sulci in theories of aging and development, (2) emphasizing the importance of individual-level investigations relating to brain structure and cognition, (3) describing structural brain changes differentiating aging and AD, and (4) discussing limitations and future directions of this work.

Our finding that age- and AD-related atrophy is most prominent in small, shallow sulci highlights the importance of investigating these often-overlooked structures. While sulci are categorized as primary, secondary, and tertiary based on their emergence in gestation, tertiary sulci are generally the smallest and shallowest cortical indentations (Sanides, 1964; Miller et al., 2021; Miller and Weiner, 2022); therefore, in the absence of ontogenetic studies including these small, newly uncovered sulci, we refer to these shallow indentations as "putative" tertiary sulci.

The findings of this study relate to classical theories of brain aging and development. The retrogenesis or "last in, first out" model proposes that brain aging mirrors development, with the latest-developing and evolutionarily newest brain structures (e.g., prefrontal cortex and association cortices more generally) being the first to degenerate (Reisberg et al., 1999). This theory has also been applied to cognition, with the observation that later-developing cognitive functions (e.g., executive function) decline first with age. In line with this hypothesis, we find that in PMC, these shallow putative tertiary sulci show the

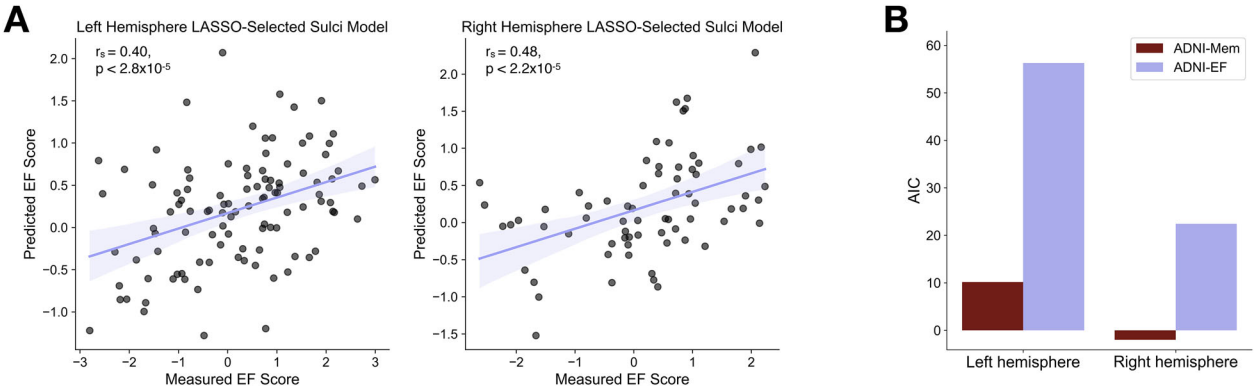

Figure 5. The thickness of LASSO-selected sulci in both hemispheres are associated with ADNI-EF scores. ***A***, Spearman's correlation (r_s) between actual and predicted ADNI-EF composite scores from a linear regression model using LASSO-selected PMC sulcal thickness to predict ADNI-EF scores instead of ADNI-Mem composite scores (Fig. 4), for both hemispheres. ***B***, Model comparison (AIC) of LASSO-selected sulci thickness models predicting ADNI-EF scores and ADNI-Mem scores; ADNI-Mem thickness models have substantially lower AICs in both cases than ADNI-EF models, and both right hemisphere models have lower AICs than left hemisphere models. See Extended Data Figure 5-1 for ADNI-Mem and ADNI-EF score distributions.

most atrophy in aging and AD, suggesting that tertiary sulci may provide structural evidence to support this theory. In addition, a classic neuroanatomical hypothesis proposes that morphological changes in tertiary sulci are likely to be associated with development of higher-order cognitive skills (Sanides, 1964). A growing body of evidence across ages, species, and clinical populations supports this theory (Garrison et al., 2015; Hopkins et al., 2021; Voorhies et al., 2021; Harper et al., 2022; Willbrand et al., 2022b, 2023a; Yao et al., 2022). Combining this theory with the retrogenesis model suggests that these tertiary-prominent morphological changes may also be related to cognitive decline in aging. Our findings somewhat support this link, as the small, shallow sulci that show the greatest atrophy are among the sulci with the strongest and most consistent relationships to cognitive decline in PMC.

Investigating sulcal morphology in aging and AD at the individual level has distinct advantages. For example, applying the retrogenesis hypothesis to global cortical atrophy and demyelination patterns has shown mixed results (Raz, 2005; Brickman et al., 2012). Our results suggest that investigating brain structure on a finer anatomical scale may provide additional insights not captured by these previous studies. Furthermore, other studies investigating large-scale brain changes in sulci in aging have found that sulci are particularly vulnerable to atrophy compared with gyri (Lin et al., 2021) and that sulcal morphology relates to cognitive decline in aging and AD (Liu et al., 2011; Bertoux et al., 2019; Mortamais et al., 2022), but these investigations have all focused on global sulcal morphology or the largest, most prominent sulci. Substantial individual variability (including many tertiary sulci) is lost when relying on averaged templates and large group comparisons (Bertoux et al., 2019; Miller et al., 2021; Voorhies et al., 2021), suggesting that individual-level investigations of sulcal morphology can provide unprecedented insight into structural brain changes. This is the first study to focus on all sulci—tertiary included—in individual hemispheres across ages and AD in a cortical region, uncovering unique relationships among sulcal types and specific sulci. Extending these methods to additional regions in future studies is an intriguing avenue to examine individual-level structural changes in other areas as well as correlations of sulcal changes across the brain at the level of individually defined sulci.

Analyzing sulcal morphology in aging and AD can also provide insight into mechanistic links between structural changes and cognitive decline. Previously reported links between tertiary sulcal morphology and the development of cognitive skills have been proposed to reflect differences in neural efficiency due to underlying white matter connectivity differences (Garrison et al., 2015; Voorhies et al., 2021). In aging, sulcal changes (e.g., in width and depth) in the most prominent sulci across the cortex have been associated with decreases in white matter volume (Im et al., 2008; Liu et al., 2013). These findings have not been extended to include tertiary sulci, which future research could explore.

Relatedly, improving our understanding of structural changes in the aging brain could aid in differentiating atrophy patterns in healthy aging and AD. Prior work has found that the morphology (including sulcal cortical thickness) of several large, prominent sulci more accurately predicts AD diagnosis than more traditional MRI metrics such as hippocampal volume, cortical thickness, and regional volume (of several regions, including precuneus and posterior cingulate gyri; Bertoux et al., 2019). Including tertiary sulci could further improve the accuracy of such predictive models. Additionally, specific tertiary sulci have been found to have translational applications; for example, the absence of the variable paracingulate sulcus is associated with a reduction of age of onset of behavioral variant frontotemporal dementia (Harper et al., 2022), and paracingulate sulcal length is inversely associated with likelihood of hallucinations in schizophrenia (Garrison et al., 2015). Investigating the diagnostic potential of these variable tertiary sulci is thus another intriguing avenue for future work, as is investigating relationships between their morphology and pathology. Postmortem histological studies suggest that Aβ accumulates in sulci more than gyri (Gentleman et al., 1992; Clinton et al., 1993), but these findings have not been investigated in tertiary sulci or with in vivo imaging methods such as PET imaging, which is another potential line of future research.

An additional topic of future study is investigating hemispheric differences reported here: right hemisphere sulci were thicker and shallower, and right hemisphere sulcal thickness was most associated with cognition. While global hemispheric differences in atrophy in aging and AD are not established, these findings in PMC are in line with previous work reporting lower cortical volume between MCI/AD and controls in right (but not left) precuneus and parietal regions and lower cortical thickness in the right isthmus cingulate in AD

versus MCI (Bertoux et al., 2019). Future work may examine whether these hemispheric differences in sulcal morphology and atrophy are consistent across the cortex, or if they are specific to PMC.

A limitation of the present study is the time-consuming process of manually labeling sulci in individual hemispheres, which limits the feasible sample size. The 4,362 sulci in 432 hemispheres across three groups are a large sample size for an anatomical–cognitive study, but a relatively small sample size compared with studies investigating group-level, cortex-wide structural changes in aging averaging across hundreds of participants. Ongoing work is underway to develop deep learning algorithms to accurately define tertiary sulci automatically in individual participants in the lateral prefrontal cortex (LPFC; Lyu et al., 2021), PMC (Willbrand et al., 2022a), and the whole brain (Borne et al., 2020). Additionally, the age- and AD-related atrophy patterns reported here are cross-sectional. Future work is underway to extend these findings to longitudinal investigations of sulcal atrophy. Recent results showing a relationship between longitudinal morphological changes in LPFC sulci and longitudinal changes in cognition in individual participants (age 6–18) show promise for this endeavor (Willbrand et al., 2023a). Another limitation is the lack of ontogenetic data to definitively characterize these small, shallow sulci as tertiary. In addition to this limitation, it is important to note that uncovering the source of vulnerability of these putative tertiary sulci cannot be fully addressed in this work and should be the focus of future studies. For example, the size, developmental trajectory, or localization in brain regions associated with pathology (e.g., Aβ and tau) could all contribute to this vulnerability—extending investigations to other areas of the brain where these factors can be distinguished will help address these questions.

In summary, we manually identified PMC sulci in individual participants and demonstrated that small, shallow putative tertiary sulci in this region atrophy more than larger sulci in aging and AD. A subset of these sulci is also associated with cognitive decline. We connect these findings to theoretical explanations of brain aging and highlight the importance of extending anatomical investigations to include individual-level sulcal analyses. These results bolster mechanistic and theoretical insights regarding structural changes in brain aging and serve as a foundation for future work further examining unique properties of tertiary sulci in aging and AD.

References

Amiez C, et al. (2023) A revised perspective on the evolution of the lateral frontal cortex in primates. Sci Adv 9:eadf9445.

Amiez C, Sallet J, Hopkins WD, Meguerditchian A, Hadj-Bouziane F, Ben Hamed S, Wilson CRE, Procyk E, Petrides M (2019) Sulcal organization in the medial frontal cortex provides insights into primate brain evolution. Nat Commun 10:3437.

Amiez C, Wilson CRE, Procyk E (2018) Variations of cingulate sulcal organization and link with cognitive performance. Sci Rep 8:13988.

Andrews-Hanna JR, Snyder AZ, Vincent JL, Lustig C, Head D, Raichle ME, Buckner RL (2007) Disruption of large-scale brain systems in advanced aging. Neuron 56:924–935.

Armstrong E, Schleicher A, Omran H, Curtis M, Zilles K (1995) The ontogeny of human gyrification. Cereb Cortex 5:56–63.

Bertoux M, et al. (2019) Sulcal morphology in Alzheimer's disease: an effective marker of diagnosis and cognition. Neurobiol Aging 84:41–49.

Borne L, Rivière D, Mancip M, Mangin J-F (2020) Automatic labeling of cortical sulci using patch- or CNN-based segmentation techniques combined with bottom-up geometric constraints. Med Image Anal 62:101651.

Borst G, Cachia A, Tissier C, Ahr E, Simon G, Houdé O (2016) Early cerebral constraints on reading skills in school-age children: an MRI study. Mind Brain Educ 10:47–54.

Braak H, Braak E (1991) Neuropathological stageing of Alzheimer-related changes. Acta Neuropathol (Berl) 82:239–259.

Brickman AM, Meier IB, Korgaonkar MS, Provenzano FA, Grieve SM, Siedlecki KL, Wasserman BT, Williams LM, Zimmerman ME (2012) Testing the white matter retrogenesis hypothesis of cognitive aging. Neurobiol Aging 33:1699–1715.

Buckner RL, Sepulcre J, Talukdar T, Krienen FM, Liu H, Hedden T, Andrews-Hanna JR, Sperling RA, Johnson KA (2009) Cortical hubs revealed by intrinsic functional connectivity: mapping, assessment of stability, and relation to Alzheimer's disease. J Neurosci 29:1860–1873.

Cachia A, Del Maschio N, Borst G, Della Rosa PA, Pallier C, Costa A, Houdé O, Abutalebi J (2017) Anterior cingulate cortex sulcation and its differential effects on conflict monitoring in bilinguals and monolinguals. Brain Lang 175:57–63.

Chi JG, Dooling EC, Gilles FH (1977) Gyral development of the human brain. Ann Neurol 1:86–93.

Chiavaras MM, Petrides M (2000) Orbitofrontal sulci of the human and macaque monkey brain. J Comp Neurol 422:35–54.

Clinton J, Roberts GW, Gentleman SM, Royston MC (1993) Differential pattern of β-amyloid protein deposition within cortical sulci and gyri in Alzheimer's disease. Neuropathol Appl Neurobiol 19:277–281.

Crane PK, et al. (2012) Development and assessment of a composite score for memory in the Alzheimer's Disease Neuroimaging Initiative (ADNI). Brain Imaging Behav 6:502–516.

Dale AM, Fischl B, Sereno MI (1999) Cortical surface-based analysis. I. Segmentation and surface reconstruction. NeuroImage 9:179–194.

Demirci N, Holland MA (2022) Cortical thickness systematically varies with curvature and depth in healthy human brains. Hum Brain Mapp 43:2064–2084.

Du A-T, Schuff N, Kramer JH, Rosen HJ, Gorno-Tempini ML, Rankin K, Miller BL, Weiner MW (2007) Different regional patterns of cortical thinning in Alzheimer's disease and frontotemporal dementia. Brain J Neurol 130:1159–1166.

Edde M, Dilharreguy B, Theaud G, Chanraud S, Helmer C, Dartigues J-F, Amieva H, Allard M, Descoteaux M, Catheline G (2020) Age-related change in episodic memory: role of functional and structural connectivity between the ventral posterior cingulate and the parietal cortex. Brain Struct Funct 225:2203–2218.

Fischl B, Dale AM (2000) Measuring the thickness of the human cerebral cortex from magnetic resonance images. Proc Natl Acad Sci 97: 11050–11055.

Fischl B, Sereno MI, Dale AM (1999a) Cortical surface-based analysis. II: inflation, flattening, and a surface-based coordinate system. NeuroImage 9:195–207.

Fischl B, Sereno MI, Tootell RB, Dale AM (1999b) High-resolution intersubject averaging and a coordinate system for the cortical surface. Hum Brain Mapp 8:272–284.

Fjell AM, et al. (2009b) High consistency of regional cortical thinning in aging across multiple samples. Cereb Cortex 19:2001–2012.

Fjell AM, Walhovd KB, Fennema-Notestine C, McEvoy LK, Hagler DJ, Holland D, Brewer JB, Dale AM (2009a) One-year brain atrophy evident in healthy aging. J Neurosci 29:15223–15231.

Foster BL, Koslov SR, Aponik-Gremillion L, Monko ME, Hayden BY, Heilbronner SR (2023) A tripartite view of the posterior cingulate cortex. Nat Rev Neurosci 24:173–189.

Garrison JR, Fernyhough C, McCarthy-Jones S, Haggard M, Simons JS (2015) Paracingulate sulcus morphology is associated with hallucinations in the human brain. Nat Commun 6:8956.

Gentleman SM, Allsop D, Bruton CJ, Jagoe R, Polak JM, Roberts GW (1992) Quantitative differences in the deposition of beta A4 protein in the sulci and gyri of frontal and temporal isocortex in Alzheimer's disease. Neurosci Lett 136:27–30.

Gibbons LE, Carle AC, Mackin RS, Harvey D, Mukherjee S, Insel P, Curtis SM, Mungas D, Crane PK, Alzheimer's Disease Neuroimaging Initiative (2012) A composite score for executive functioning, validated in Alzheimer's Disease Neuroimaging Initiative (ADNI) participants with baseline mild cognitive impairment. Brain Imaging Behav 6: 517–527.

Glasser MF, et al. (2013) The minimal preprocessing pipelines for the human connectome project. NeuroImage 80:105–124.

Goghari VM, Rehm K, Carter CS, Macdonald AW (2007) Sulcal thickness as a vulnerability indicator for schizophrenia. Br J Psychiatry 191:229–233.
Hamelin L, et al. (2015) Sulcal morphology as a new imaging marker for the diagnosis of early onset Alzheimer's disease. Neurobiol Aging 36:2932–2939.
Harper L, et al. (2022) Prenatal gyrification pattern affects age at onset in frontotemporal dementia. Cereb Cortex 32:3937–3944.
Harrison TM, et al. (2019) Longitudinal tau accumulation and atrophy in aging and Alzheimer disease. Ann Neurol 85:229–240.
Heinze G, Wallisch C, Dunkler D (2018) Variable selection - a review and recommendations for the practicing statistician. Biom J Biom Z 60:431–449.
Hopkins WD, Procyk E, Petrides M, Schapiro SJ, Mareno MC, Amiez C (2021) Sulcal morphology in cingulate cortex is associated with voluntary oro-facial motor control and gestural communication in chimpanzees (Pan troglodytes). Cereb Cortex 31:2845–2854.
Im K, Lee J-M, Seo SW, Hyung Kim S, Kim SI, Na DL (2008) Sulcal morphology changes and their relationship with cortical thickness and gyral white matter volume in mild cognitive impairment and Alzheimer's disease. NeuroImage 43:103–113.
Jack CR, et al. (2008) The Alzheimer's Disease Neuroimaging Initiative (ADNI): MRI methods. J Magn Reson Imaging 27:685–691.
Jin K, Zhang T, Shaw M, Sachdev P, Cherbuin N (2018) Relationship between sulcal characteristics and brain aging. Front Aging Neurosci 10:339.
Landau SM, Mintun MA, Joshi AD, Koeppe RA, Petersen RC, Aisen PS, Weiner MW, Jagust WJ, Alzheimer's Disease Neuroimaging Initiative (2012) Amyloid deposition, hypometabolism, and longitudinal cognitive decline. Ann Neurol 72:578–586.
Leech R, Sharp DJ (2014) The role of the posterior cingulate cortex in cognition and disease. Brain 137:12–32.
Lin H-Y, Huang C-C, Chou K-H, Yang AC, Lo C-YZ, Tsai S-J, Lin C-P (2021) Differential patterns of gyral and sulcal morphological changes during normal aging process. Front Aging Neurosci 13:625931.
Lindroth H, Nair VA, Stanfield C, Casey C, Mohanty R, Wayer D, Rowley P, Brown R, Prabhakaran V, Sanders RD (2019) Examining the identification of age-related atrophy between T1 and T1+T2-FLAIR cortical thickness measurements. Sci Rep 9:11288.
Liu T, et al. (2013) Limited relationships between two-year changes in sulcal morphology and other common neuroimaging indices in the elderly. NeuroImage 83:12–17.
Liu T, Wen W, Zhu W, Kochan NA, Trollor JN, Reppermund S, Jin JS, Luo S, Brodaty H, Sachdev PS (2011) The relationship between cortical sulcal variability and cognitive performance in the elderly. NeuroImage 56:865–873.
Lopez-Persem A, Verhagen L, Amiez C, Petrides M, Sallet J (2019) The human ventromedial prefrontal cortex: sulcal morphology and its influence on functional organization. J Neurosci 39:3627–3639.
Lyu I, Bao S, Hao L, Yao J, Miller JA, Voorhies W, Taylor WD, Bunge SA, Weiner KS, Landman BA (2021) Labeling lateral prefrontal sulci using spherical data augmentation and context-aware training. NeuroImage 229:117758.
Madan CR (2019) Robust estimation of sulcal morphology. Brain Inform 6:5.
Mangin J-F, Poupon F, Duchesnay E, Rivière D, Cachia A, Collins DL, Evans AC, Régis J (2004) Brain morphometry using 3D moment invariants. Med Image Anal 8:187–196.
Miller JA, Voorhies WI, Lurie DJ, Esposito D, Weiner M, S K (2021) Overlooked tertiary sulci serve as a meso-scale link between microstructural and functional properties of human lateral prefrontal cortex. J Neurosci 41:2229–2244.
Miller JA, Weiner KS (2022) Unfolding the evolution of human cognition. Trends Cogn Sci 26:735–737.
Mortamais M, et al. (2022) Sulcal morphology as cognitive decline predictor in older adults with memory complaints. Neurobiol Aging 113:84–94.
Parvizi J, Van Hoesen GW, Buckwalter J, Damasio A (2006) Neural connections of the posteromedial cortex in the macaque. Proc Natl Acad Sci 103:1563–1568.
Pengas G, Hodges JR, Watson P, Nestor PJ (2010) Focal posterior cingulate atrophy in incipient Alzheimer's disease. Neurobiol Aging 31:25–33.
Petersen RC, et al. (2010) Alzheimer's Disease Neuroimaging Initiative (ADNI): clinical characterization. Neurology 74:201–209.
Petrides M (2019) *Atlas of the morphology of the human cerebral cortex on the average MNI brain*, Ed. 1. Academic Press. Available at: https://www.elsevier.com/books/atlas-of-the-morphology-of-the-human-cerebral-cortex-on-the-average-mni-brain/petrides/978-0-12-800932-1 [Accessed June 20, 2022].
Raz N (2005) Ageing and the brain. In: *Encyclopedia of life sciences,* John Wiley & Sons, Ltd. Available at: https://onlinelibrary.wiley.com/doi/abs/10.1038/npg.els.0004063 [Accessed July 3, 2022].
Raz N, Gunning FM, Head D, Dupuis JH, McQuain J, Briggs SD, Loken WJ, Thornton AE, Acker JD (1997) Selective aging of the human cerebral cortex observed in vivo: differential vulnerability of the prefrontal gray matter. Cereb Cortex 7:268–282.
Reisberg B, Franssen EH, Hasan SM, Monteiro I, Boksay I, Souren LEM, Kenowsky S, Auer SR, Elahi S, Kluger A (1999) Retrogenesis: clinical, physiologic, and pathologic mechanisms in brain aging, Alzheimer's and other dementing processes. Eur Arch Psychiatry Clin Neurosci 249:S28–S36.
Royse SK, Minhas DS, Lopresti BJ, Murphy A, Ward T, Koeppe RA, BullichS, DeSanti S, Jagust WJ, Landau SM, Alzheimer's Disease Neuroimaging Initiative (2021) Validation of amyloid PET positivity thresholds in centiloids: a multisite PET study approach. Alzheimers Res Ther 13:99.
Salat DH, Buckner RL, Snyder AZ, Greve DN, Desikan RSR, Busa E, Morris JC, Dale AM, Fischl B (2004) Thinning of the cerebral cortex in aging. Cereb Cortex 14:721–730.
Sanides F (1964) Structure and function of the human frontal lobe. Neuropsychologia 2:209–219.
Shen X, et al. (2018) Variation in longitudinal trajectories of cortical sulci in normal elderly. NeuroImage 166:1–9.
Tang H, Liu T, Liu H, Jiang J, Cheng J, Niu H, Li S, Brodaty H, Sachdev P, Wen W (2021) A slower rate of sulcal widening in the brains of the non-demented oldest old. NeuroImage 229:117740.
Vandekar SN, et al. (2015) Topologically dissociable patterns of development of the human cerebral cortex. J Neurosci 35:599–609.
Van Essen DC (2020) A 2020 view of tension-based cortical morphogenesis. Proc Natl Acad Sci U S A. 117:32868–32879.
Van Essen DC, Smith SM, Barch DM, Behrens TEJ, Yacoub E, Ugurbil K (2013) The WU-Minn Human Connectome Project: an overview. NeuroImage 80:62–79.
Vannini P, Hedden T, Huijbers W, Ward A, Johnson KA, Sperling RA (2013) The ups and downs of the posteromedial cortex: age- and amyloid-related functional alterations of the encoding/retrieval flip in cognitively normal older adults. Cereb Cortex 23:1317–1328.
Vogt BA, Nimchinsky EA, Vogt LJ, Hof PR (1995) Human cingulate cortex: surface features, flat maps, and cytoarchitecture. J Comp Neurol 359:490–506.
Voorhies WI, Miller JA, Yao JK, Bunge SA, Weiner KS (2021) Cognitive insights from tertiary sulci in prefrontal cortex. Nat Commun 12:5122.
Welker W (1990) Why does cerebral cortex fissure and fold? In: *Cerebral cortex: comparative structure and evolution of cerebral cortex, Part II* (Jones EG, Peters A, eds), pp 3–136. Cerebral Cortex. Boston, MA: Springer US. Available at: https://doi.org/10.1007/978-1-4615-3824-0_1 [Accessed August 1, 2021].
Westman E, Aguilar C, Muehlboeck J-S, Simmons A (2013) Regional magnetic resonance imaging measures for multivariate analysis in Alzheimer's disease and mild cognitive impairment. Brain Topogr 26:9–23.
Willbrand EH, et al. (2022a) Uncovering a tripartite landmark in posterior cingulate cortex. Sci Adv 8:eabn9516.
Willbrand EH, Ferrer E, Bunge SA, Weiner KS (2023a) Development of human lateral prefrontal sulcal morphology and its relation to reasoning performance. J Neurosci 43:2552–2567.
Willbrand EH, Jackson S, Chen S, Hathaway CB, Voorhies WI, Bunge SA, Weiner KS (2023b) Sulcal variability in anterior lateral prefrontal cortex contributes to variability in reasoning performance among young adults. bioRxiv.
Willbrand EH, Maboudian SA, Kelly JP, Parker BJ, Foster BL, Weiner KS (2023c) Sulcal morphology of posteromedial cortex substantially differs between humans and chimpanzees. Commun Biol 6:1–14.
Willbrand EH, Voorhies WI, Yao JK, Weiner KS, Bunge SA (2022b) Presence or absence of a prefrontal sulcus is linked to reasoning performance during child development. Brain Struct Funct 227:2543–2551.
Yao JK, Voorhies WI, Miller JA, Bunge SA, Weiner KS (2022) Sulcal depth in prefrontal cortex: a novel predictor of working memory performance. Cereb Cortex 33:1799–1813.
Zilles K, Palomero-Gallagher N, Amunts K (2013) Development of cortical folding during evolution and ontogeny. Trends Neurosci 36:275–284.